Electronic Supplementary Material (ESI) for Nanoscale Horizons.

Supporting Information

White luminescent single-crystalline chlorinated graphene quantum dots

Weitao Li, Huazhang Guo, Gao Li, Zhen Chi, Hailong Chen, Liang Wang, Yijian Liu, Keng Chen, Mengying Le, Yu Han, Luqiao Yin, Robert Vajtai, Pulickel M Ajayan, Yuxiang Weng and Minghong Wu

1. Experimental Procedures

1.1 Synthesis of WGQDs. Typically, 4.0 mL of TCM was dissolved in 6 mL ethanol, and then 100 mg of DAN was added into the solvent under ultrasonic conditions. The as-formed homogeneous solution was transferred to a reactor of Teflon (25 mL) and heated at 230 ^{o}C for 12 h to synthesize the WGQDs. Synthesis of other control experimental WGQDs was regulated in different volume ratios (ranging from 10:0 to 5:5 (ethanol: TCM)). Simultaneously, the WGQDs were also synthesized at different temperatures (180-230 ^{o}C) and under the same solvent conditions (6:4). After cooling, the mixture colloids were subjected to dialysis (MWCO: 3500 Da) for three days and dried at 60 ^{o}C for structural characterization. For optical and applications, the resultant WGQDs were directly used without purification.

For reference, the GQDs without Cl-dopant were synthesized under lacking TCM in the same preparation process of WGQDs, which denoted No-Cl-GQDs, and another comparison GQDs named Lt-GQDs was manufactured at low-temperature of 180 ^{o}C in the similar preparation process of WGQDs.

1.2 Material Characterization. Transmission electron microscopy (TEM) was performed on a JEM-2100F electron microscope operating at 200 kV. Atomic force microscopy (AFM) images were taken using an SPM-9600 AFM. X-ray direction (XRD) patterns were obtained with a Rigaku 18 KW D/max-2550 with Cu Kα radiation. Absorption, fluorescence, and phosphorescence were registered using a Hitachi 3100 spectrophotometer and a Hitachi 7000 fluorescence spectrophotometer. FTIR spectrum were recognized with a Bio-Rad FTIR spectrometer FTS165. Raman spectra were recorded on a Micro Raman spectrometer (Thermo Scientific DXR) with λ_{ex} = 633 nm. XPS spectra were gathered using a Kratoms Axis Ultra DLD X-ray photoelectron spectrometer.

1.3 Preparation of WLEDs. The WGQDs (150 μL, 15 mg·mL^{-1}) was added to 1.6 g of ET-821A silica gel and 0.4 g of ET-821B silica gel, and then the mixture was stirred for 15 minutes (50 r·min^{-1}). After that the mixture of WGQDs was added dropwise to a UV-ray chip device with emission wavelength at 390 nm, then the device was dried in an oven at 80 ^{o}C for 30 minutes.

1.4 Method of Bioimaging. HeLa cells were cultured according to previous study.[1] Interestingly, the cells were examined under a confocal microscope (Leica TCS SP5) using lasers of 405, 488, 514, 543, and 633 nm. To determine the nuclear targeting of WGQDs, we also use DAPI dye (Keygen Institute of Biotechnology, China) with a concentration of 2 μg·mL^{-1} to stain the nucleus of HeLa cells.

1.5 UPS Measurement. UPS measurement was performed with an *hv*=21.22 eV, He I source (ESCALAB 250XI, Thermo). The WGQDs thin films were prepared from spin-coating on indium tin oxide (ITO) substrates for UPS measurement.

2. Figures S1-S25

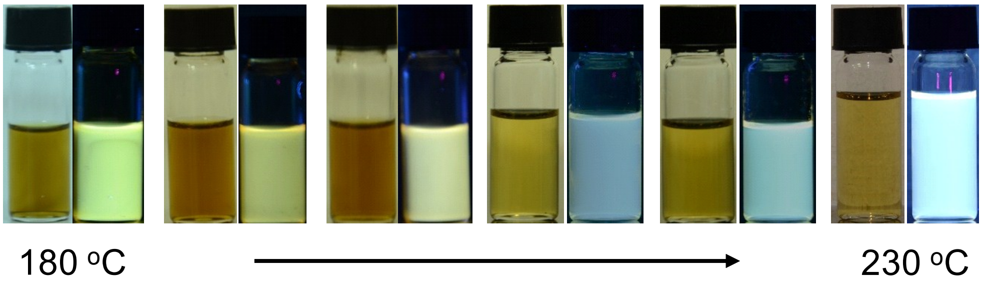

Figure S1. The photographs of GQDs prepared at different temperature. From left to right, these samples were prepared at different temperature (180-230 °C, every 10 °C interval) under daylight (left) and UV light irradiation (right).

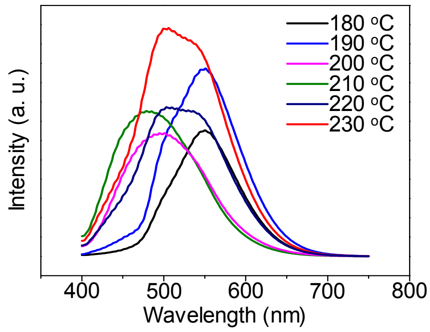

Figure S2. PL spectra of GQDs synthesized at different temperature (180-230 °C).

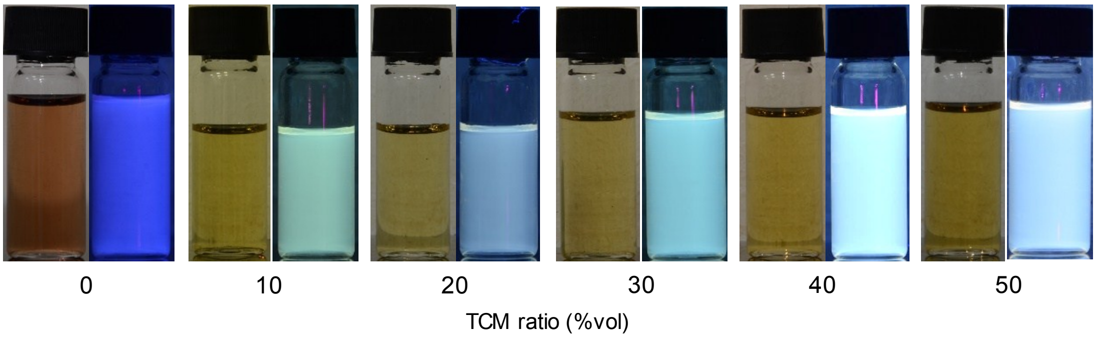

Figure S3. The photographs of GQDs synthesized in ethanol solution contained different TCM volume ratio at 230 °C under daylight (left) and UV light irradiation (right).

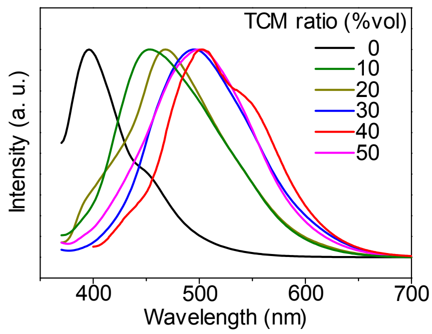

Figure S4. PL spectra of GQDs synthesized in ethanol solution contained different TCM volume ratio at 230 °C.

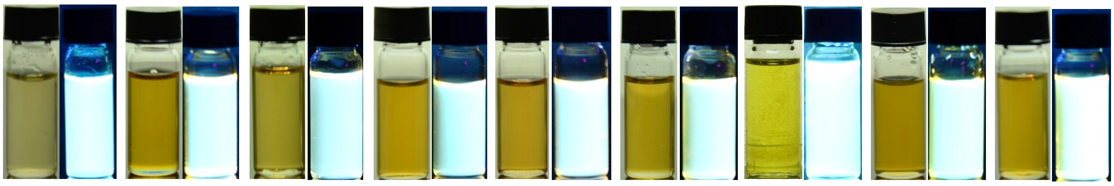

Figure S5. The photographs of WGQDs dispersed in different solvents under daylight (left) and UV light irradiation (right). The solvents are water, toluene, N,N-dimethylformamide (DMF), acetone, tetrahydrofuran (THF), dimethyl sulfoxide (DMSO), methanol (MeOH), methyl cyanide (CH3CN), and isopropanol (i-POH) from left to right.

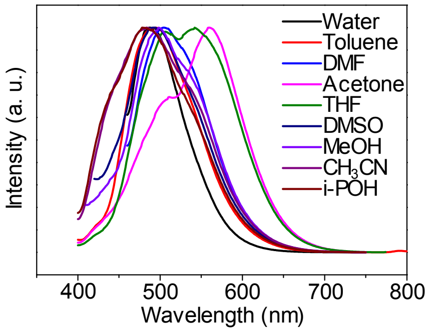

Figure S6. PL spectra of WGQDs dispersed in many solvents at different excitation wavelengths. The solvents are water, toluene, DMF, acetone, THF, DMSO, MeOH, CH_3CN, and i-POH from left to right.

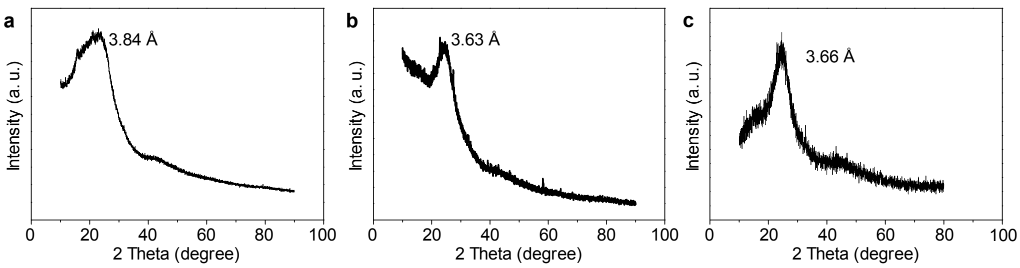

Figure S7. XRD patterns of WGQDs (a), No-Cl-GQDs (b) and Lt-GQDs (c).

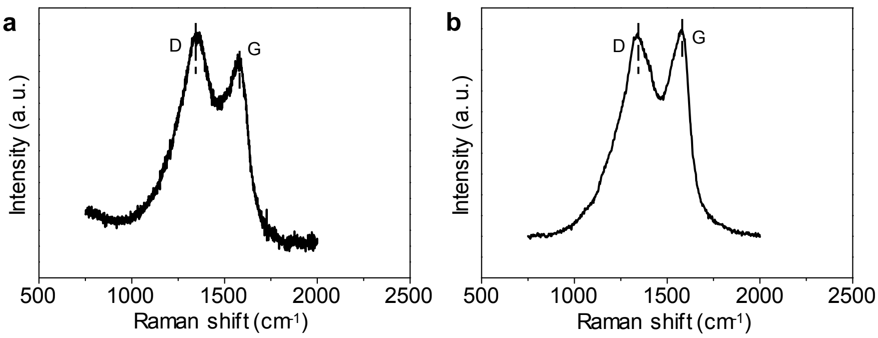

Figure S8. The typical Raman spectra of No-Cl-GQDs (a) and Lt-GQDs (b).

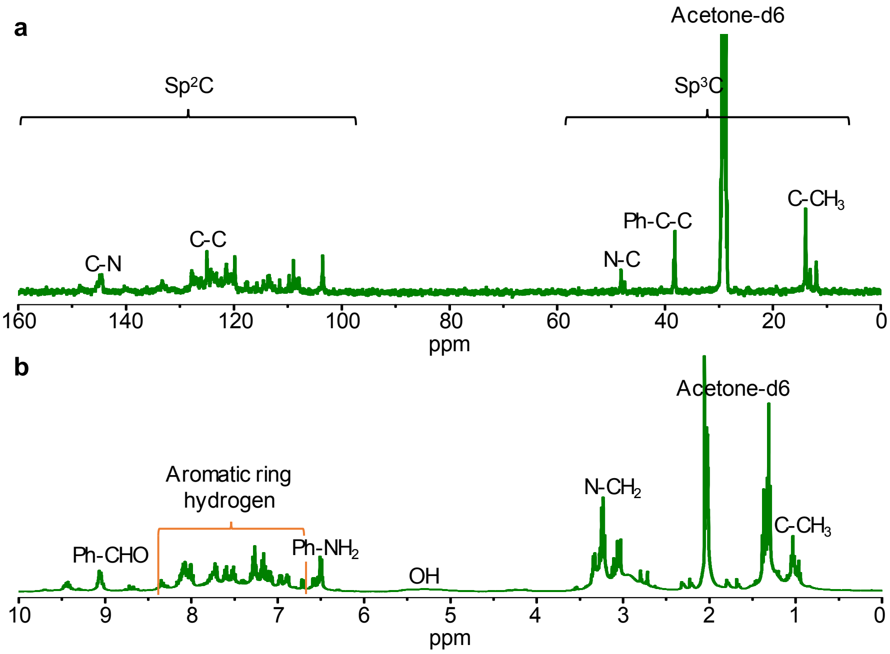

Figure S9. The NMR spectroscopy of WGQDs. ^{13}C NMR (a) and ^{1}H NMR (b) spectra of WGQDs.

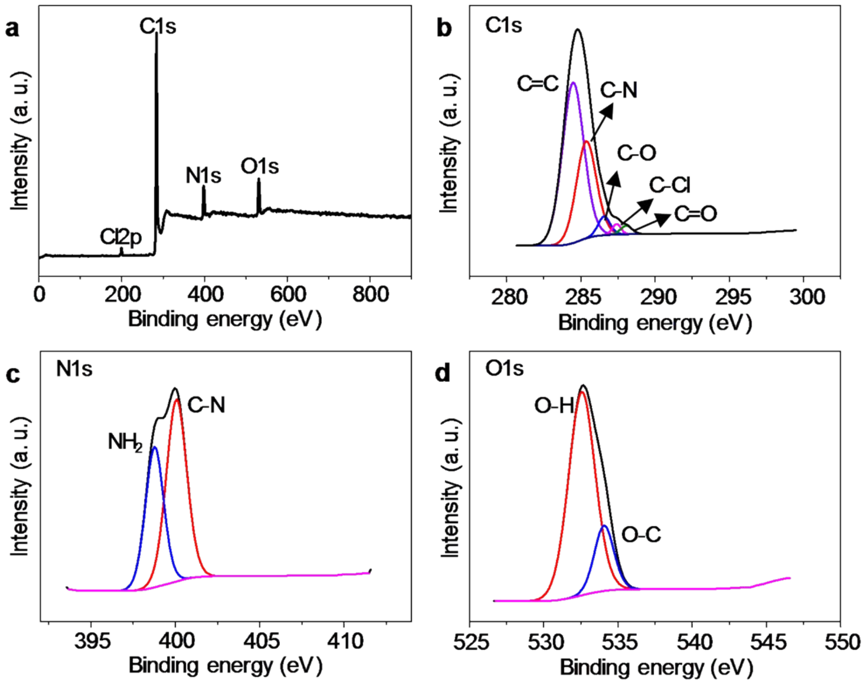

Figure S10. XPS survey and high-resolution XPS spectra of WGQDs. XPS survey spectrum (a), C1s (b), N1s (c), and O1s (d) spectra of WGQDs.

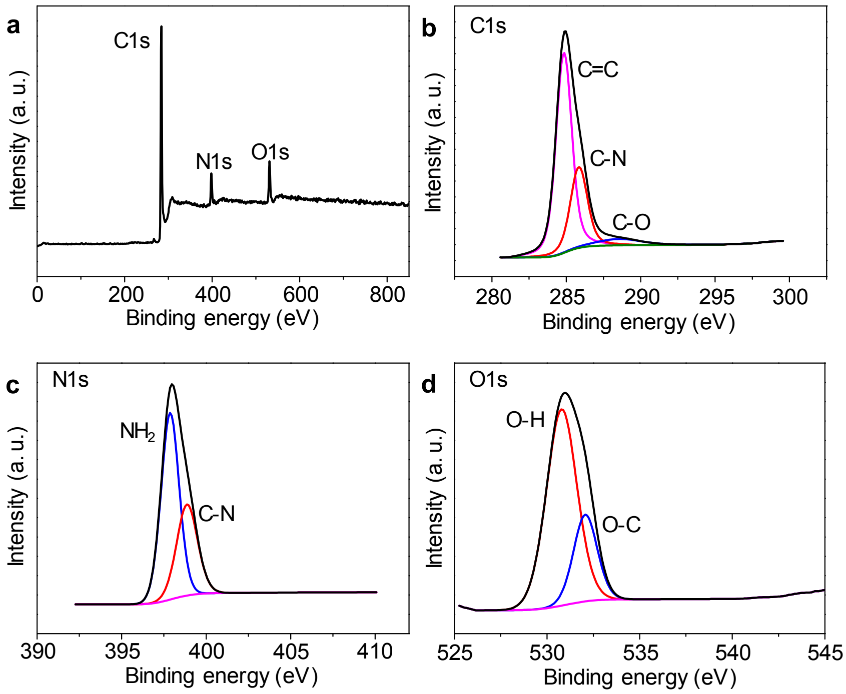

Figure S11. XPS survey and high-resolution XPS spectra of No-Cl-GQDs. XPS survey spectrum (a), C1s (b), N1s (c), and O1s (d) spectra of No-Cl-GQDs.

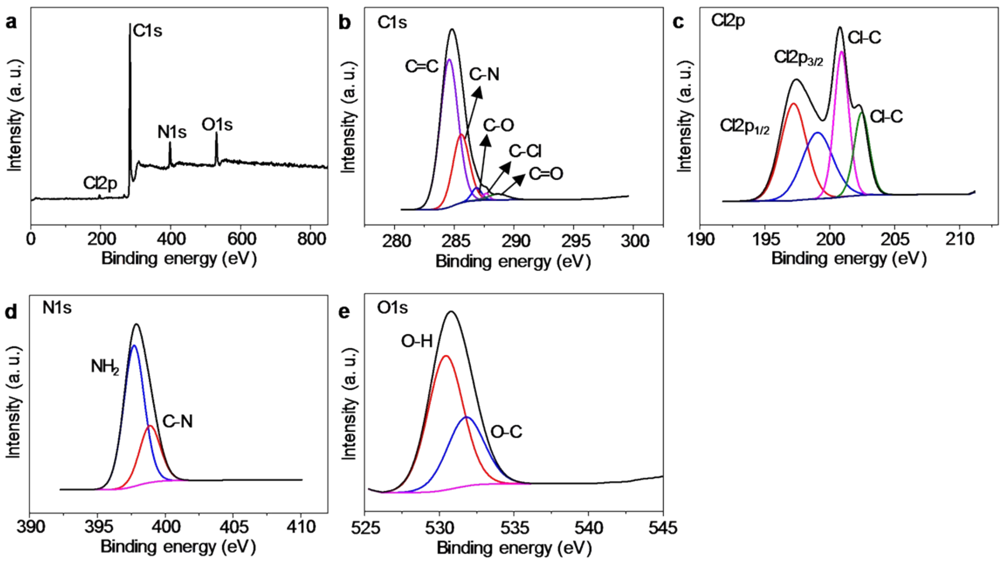

Figure S12. XPS survey and high-resolution XPS spectra of Lt-GQDs. XPS survey spectrum (a), C1s (b), Cl2p (c), N1s (d), and O1s (e) spectra of Lt-GQDs.

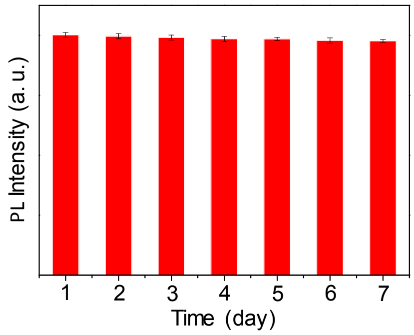

Figure S13. The fluorescence stability of WGQDs after one week. (3 measurements per group).

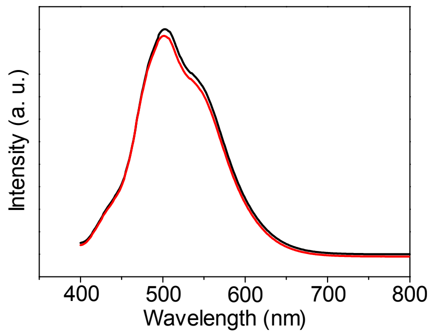

Figure S14. Colloidal stability of WGQDs via PL intensity before (black line) and after (red line) drying at 60 °C.

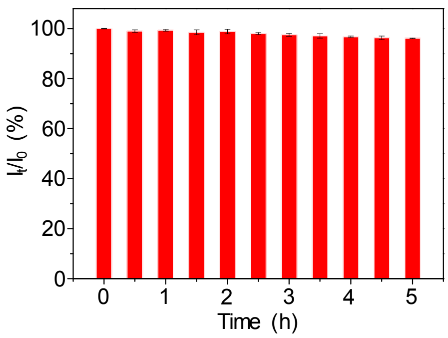

Figure S15. Photostability of WGQDs under 365 nm UV light irradiation. (3 measurements per group).

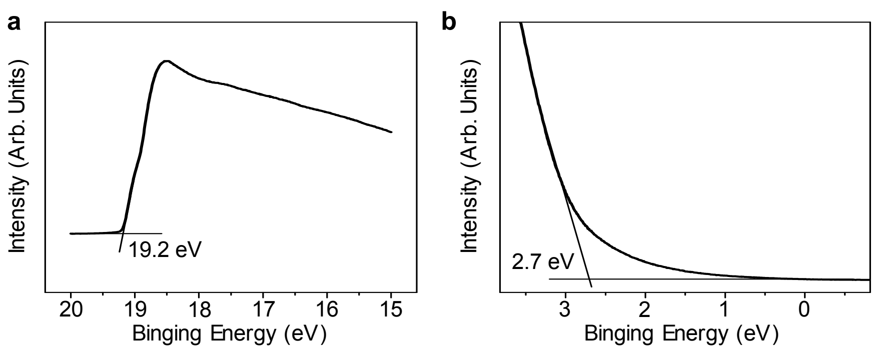

Figure S16. Ultraviolet photoelectron spectroscopy (UPS) data of WGQDs.

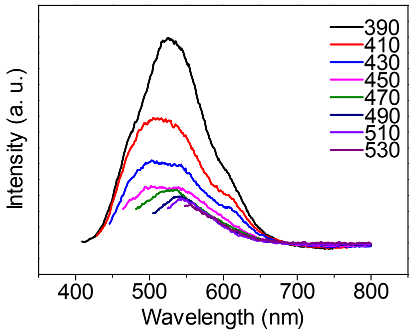

Figure S17. The phosphorescence spectra of WGQDs at different excitation wavelengths.

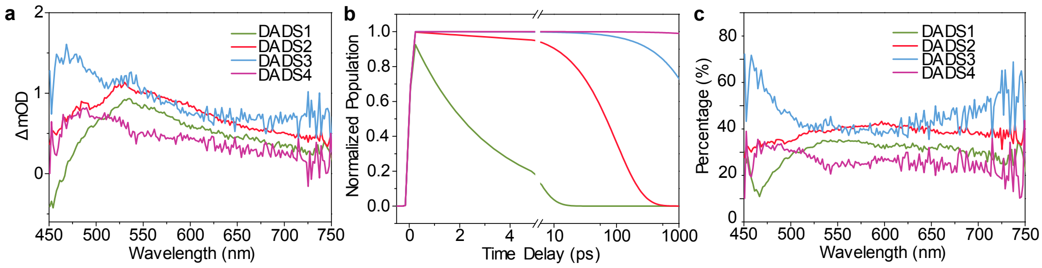

Figure S18. (a) Results of the global fitting with four exponent decay functions showing four decay associated difference spectra (DADS). (b) Results of the global fitting with four exponent decay functions showing four exponent decay dynamics with time constants 3.0 ps, 99 ps, 3.2 ns and 100 ns. The time constant of 100 ns is arbitrarily fixed during the fitting, since it is much longer than the current time window for collection and cannot be accurately determined. (c) The percentages of the four decay channels in the overall dynamics within the wavelength range constructed according to DADS.

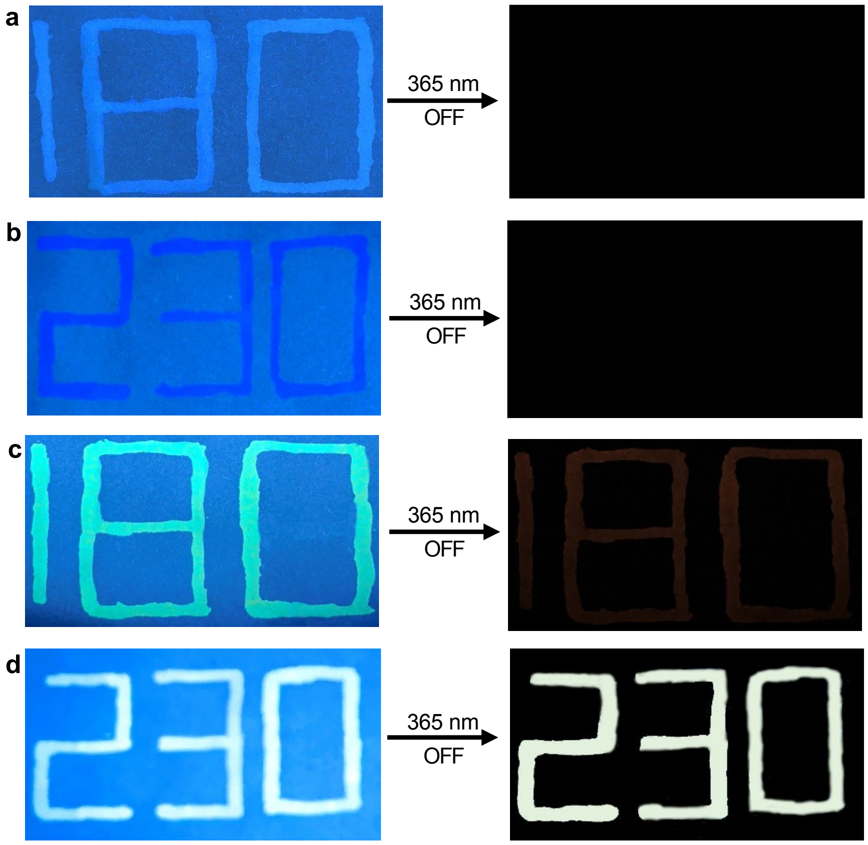

Figure S19. Phosphorescence photographs prepared by printing GQDs synthesized in ethanol solution contained different TCM volume ratio (the TCM volume ratio of a and b is 0%, the TCM volume ratio of c and d is 40%) at 180 °C (a and c) and 230 °C (b and d).

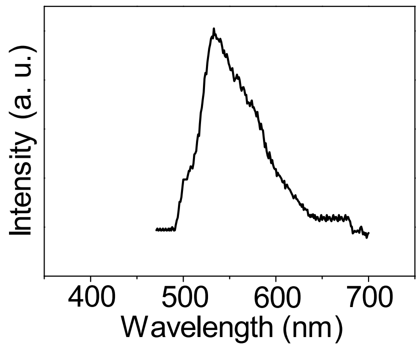

Figure S20. The phosphorescence spectrum of Lt-GQDs.

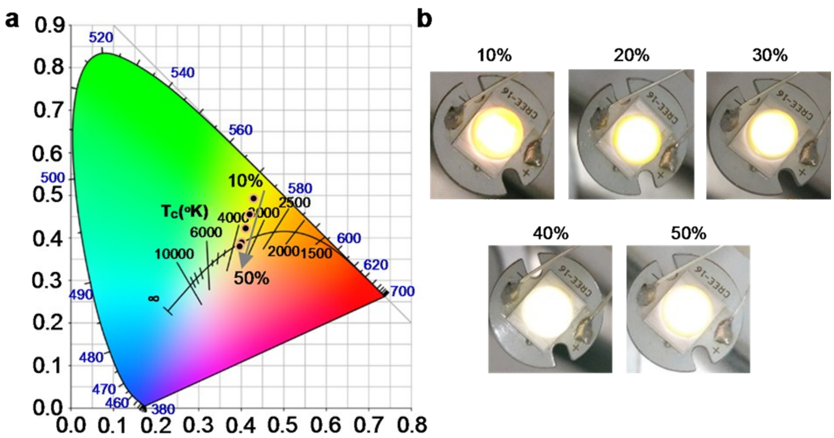

Figure S21. CIE color coordinates with different Cl doping. CIE color coordinates (a) and photographs of the WLEDs (b) with GQDs synthesized in different TCM volume ratio at 230 ºC.

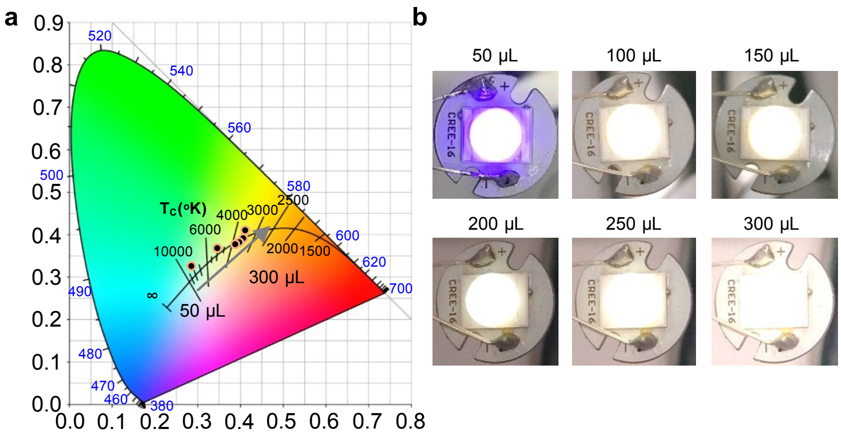

Figure S22. CIE color coordinates with different WGQDs concentration. CIE color coordinates (a) and photographs of the WLEDs (b) with different WGQDs concentration.

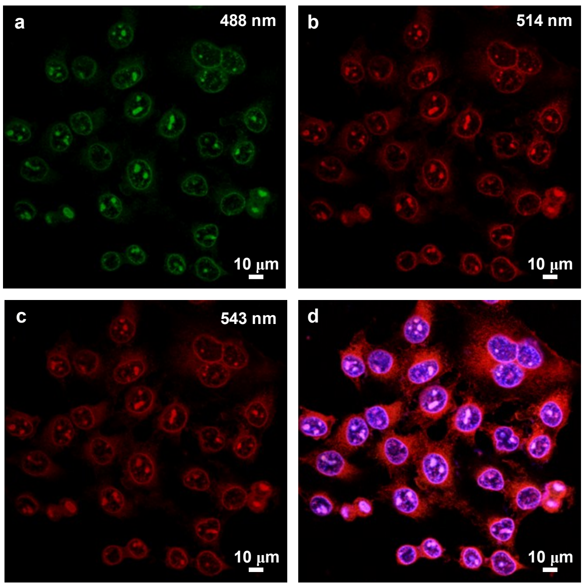

Figure S23. HeLa cells imaging with WGQDs excited at 488 nm (a), 514 nm (b), 543 nm (c) and merged all images (d).

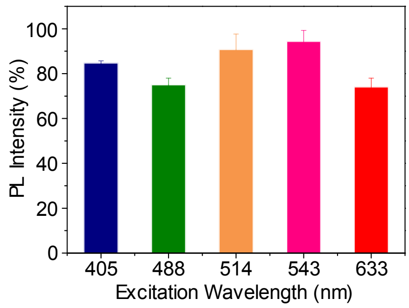

Figure S24. Fluorescence intensity analysis of HeLa cells at 405, 488, 514, 543 and 633 nm by Image J. (3 measurements per group).

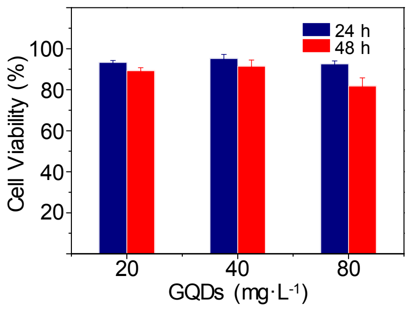

Figure S25. Cytotoxicity assessment of WGQDs at the imaging dose (20 mg L^{-1}) and higher doses for incubation time varied from 24 to 48 h using HeLa cells. (3 measurements per group)

3. Table S1-S8

Table S1. The QYs and FWHM of GQDs produced under different temperature.

Temperature (°C)	180	190	200	210	220	230
QYs (%)	30	30	31	32	33	34
FWHM (nm)	102	107	110	113	115	120

Table S2. The QYs and FWHM of GQDs produced under different ratio of TCM.

TCM volume ratio (%)	0	10	20	30	40	50
QYs (%)	6	13	17	30	34	33
FWHM (nm)	56	105	111	114	120	118

Table S3. Previous literature concerning white luminescent.

Refs.	Luminescent materials	QYs (%)	PL range (nm)	FWHM (nm)	Applications	Phosphorescence
2	hybrid semiconductor bulk materials	37	370-700	110	WLED	NO
3	Metal-Organic Frameworks	1.4	400-650	100	White-light phosphor	NO
4	Double-Layer Metal-Organic Frameworks	25.7	425-600	____	Three-color Luminescent Thermometry	NO
5	Lanthanide-based gels	3.33	475-600	____	white light emitting gel	NO
6	Covalent organic frameworks	64	400-700	120	Flexible white light emitter	NO
7	A single organic molecule	____	500-700	100	WLED	Yellow
8	Halide Post-Perovskite-Type	45	450-650	140	WLED	NO
9	GOQDs	____	400-700	80	WLED	NO
10	CDs	9.0	400-650	110	WLED	NO
11	GQDs	3.62	450-750	130	WLED	NO
12	GQDs	____	400-600	100	WLED	NO
13	CDs	35	350-550	160	WLED	NO
14	GQDs	____	400-700	110	WLED	NO
This work	GQDs	34	400-700	120	WLED, cell imaging, graphic security and information encryption	White

Table S4. The FWHM of WGQDs in the solvents.

Solvent	Ethanol	Water	Toluene	DMF	Acetone
The FWHM (nm)	120	80	100	103	127
Solvent	THF	DMSO	MeOH	CH_3CN	i-POH
The FWHM (nm)	138	111	108	137	130

Table S5. The elements ratio of WGQDs, No-Cl-GQDs and Lt-GQDs in XPS survey spectra.

Elements	Cl (%)	C (%)	O (%)	N (%)
WGQDs	2.50	82.63	7.84	7.03
No-Cl-GQDs	0	84.52	8.43	7.05
Lt-GQDs	1.32	83.43	7.88	7.37

Table S6. Previous literature concerning Cl-doping GQD/CDs.

Refs.	Cl-doping source	Cl content (at%)	Single-crystalline	I_G/I_D ratio	Fluorescent	Phosphorescence
15	Sucralose	0.89	NO	1.2	Green	NO
16	HCl	____	NO	1.05	____	NO
17	HCl	2.8	NO	1.13	White	NO
18	HCl	2	NO	____	Yellow	NO
19	HCl	3	NO	____	Blue	NO
20	HCl	0.6	NO	____	Blue	NO
21	HCl	____	NO	____	Blue	NO
22	HCl	____	NO	1.05	Blue	NO
23	HCl	____	NO	____	Blue	NO
This work	$CHCl_3$	2.5	YES	1.35	White	White

Table S7. CIE color coordinates (x, y), CRI, CCT, and luminous efficacy of WLEDs synthesized in different TCM volume ratio at 230 ^oC.

TCM volume ratio (%)	CIE (x, y)	CRI	CCT/K	Luminous efficacy (lm/W)
10	(0.42, 0.49)	67.4	3840	12.36
20	(0.41, 0.46)	72.3	3892	11.32
30	(0.40, 0.42)	72.6	3904	12.71
40	(0.39, 0.38)	70.6	3938	14.92
50	(0.39, 0.39)	73.8	3972	13.11

Table S8. CIE color coordinates (x, y), CRI, CCT, and luminous efficacy of WLEDs with different WGQDs concentration.

WGQDs volume (μL)	CIE (x, y)	CRI	CCT/K	Luminous efficacy (lm/W)
50	(0.28, 0.33)	76.3	8221	12.48
100	(0.34, 0.37)	72.3	5193	11.72
150	(0.39, 0.38)	70.6	3938	14.92
200	(0.40, 0.39)	71.9	3891	13.14
250	(0.41, 0.40)	72.0	3744	12.95
300	(0.42, 0.41)	76.1	3745	12.86

4. References

1. L. Wang, B. Wu, W. T. Li, S. L. Wang, Z. Li, M. Li, D. Y. Pan and M. H. Wu, *Adv. Biosys.*, 2018, **2**, 1700191.
2. M. Roushan, X. Zhang and J. Li, *Angew. Chem. Int. Ed.*, 2012, **51**, 436-439.
3. Y. Liu, M. Pan, Q.-Y. Yang, L. Fu, K. Li, S.-C. Wei and C.-Y. Su, *Chem. Mater.*, 2012, **24**, 1954-1960.
4. L. Qiu, C. Yu, X. Wang, Y. Xie, A. M. Kirillov, W. Huang, J. Li, P. Gao, T. Wu, X. Gu, Q. Nie and D. Wu, *Inorg. Chem.*, 2019, **58**, 4524-4533.
5. A. Sebastian, M. K. Mahato and E. Prasad, *Soft Matter*, 2019, **15**, 3407-3417.
6. S. Haldar, D. Chakraborty, B. Roy, G. Banappanavar, K. Rinku, D. Mullangi, P. Hazra, D. Kabra and R. Vaidhyanathan, *J. Am. Chem. Soc.*, 2018, **140**, 13367-13374.
7. Z. He, W. Zhao, J. W. Y. Lam, Q. Peng, H. Ma, G. Liang, Z. Shuai and B. Z. Tang, *Nat. Commun.*, 2017, **8**, 416.
8. R. Gautier, F. Massuyeau, G. Galnon and M. Paris, *Adv. Mater.*, 2019, **31**, 1807383.
9. T. Ghosh and E. Prasad, *J. Phys. Chem. C*, 2015, **119**, 2733-2742.
10. L. H. Mao, W. Q. Tang, Z. Y. Deng, S. S. Liu, C. F. Wang and S. Chen, *Ind. Eng. Chem. Res.*, 2014, **53**, 6417-6425.
11. P. Dong, B. P. Jiang, W. Q. Liang, Y. Huang, Z. J. Shi and X. C. Shen, *Inorg. Chem. Front.*, 2017, **4**, 712-718.
12. Z. M. Luo, G. Q. Qi, K. Y. Chen, M. Zou, L. H. Yuwen, X. W. Zhang, W. Huang and L. H. Wang, *Adv. Funct. Mater.*, 2016, **26**, 2739-2744.
13. Y. Chen, M. Zheng, Y. Xiao, H. Dong, H. Zhang, J. Zhuang, H. Hu, B. Lei and Y. Liu, *Adv. Mater.*, 2016, **28**, 312-318.
14. R. Sekiya, Y. Uemura, H. Murakami and T. Haino, *Angew. Chem. Int. Ed.*, 2014, **53**, 5619-5623.
15. L. F. Wang, Y. Li, Y. M. Wang, W. H. Kong, Q. P. Lu, X. G. Liu, D. W. Zhang and L. T. Qu, *ACS Appl. Mater. Interfaces*, 2019, **11**, 21822-21829.
16. J. Zhao, L. Tang, J. Xiang, R. Ji, J. Yuan, J. Zhao, R. Yu, Y. Tai and L. Song, *Appl. Phys. Lett.*, 2014, **105**, 111116.
17. X. F. Wang, G. G. Wang, J. B. Li, Z. Liu, Y. X. Chen, L. F. Liu and J. C. Han, *Chem. Eng. J.*, 2019, **361**, 773-782.
18. X. Li, S. P. Lau, L. Tang, R. Ji and P. Yang, *J. Mater. Chem. C*, 2013, **1**, 7308-7313.
19. M. Nafiujjaman, H. Joon, K. S. Kwak and Y.-k. Lee, *J. Nanosci. Nanotechnol.*, 2018, **18**, 3793-3799.
20. Y. Zhong, Q. Chen, J. Li, X. Pan, Z. Han and W. Dong, *Nano*, 2017, **12**, 1750135.
21. J. Li, K. Tang, J. Yu, H. Wang, M. Tu and X. Wang, *R. Soc. Open Sci.*, 2018, **6**, 181557.
22. J. Zhao, L. Tang, J. Xiang, R. Ji, Y. Hu, J. Yuan, J. Zhao, Y. Tai and Y. Cai, *RSC Adv.*, 2015, **5**, 29222-29229.
23. Q. Hu, T. Li, L. Gao, X. Gong, S. Rao, W. Fang, R. Gu and Z. Yang, *Sensors*, 2018, **18**, 3416.